Adsorption of Congo red onto mesoporous carbon material: equilibrium and kinetic studies

Leila Torkian[a], Behdad Ghaderi Ashtiani[b], Ehsanollah Amereh[c], Nourali Mohammadi[c],*

[a]*Department of Applied Chemistry, Islamic Azad University, South Tehran Branch, Tehran, Iran*
[b]*Department of Materials Engineering, Science and Research Campus, Islamic Azad University, Tehran, Iran*
[c]*Iranian Research & Development Center for Chemical Industries, Academic Center for Education,*
Culture and Research (ACECR), Tehran, Iran
Tel. +982614764050; Fax: +982614764051; email: norali_mohammadi@yahoo.com

ABSTRACT

In the present study, adsorption of Congo red dye on carbon mesoporous surface has been investigated. Mesoporous carbon CMK-3 adsorbent with high surface area and large pore volume was prepared and its textual and structural properties were characterized by X-ray powder diffraction patterns (XRD) and nitrogen physisorption isotherms. Adsorption experiments were carried out as batch studies at different contact time, pH, initial dye concentration and salt concentration. The dye adsorption was rapidly attained after 60 min of contact time. Removal of dye in acidic solutions was better than in basic solutions. The adsorption of dye increased with increasing initial dye concentration and salt concentration. The equilibrium data were analyzed by the Langmuir, Freundlich and Temkin models, which revealed that Langmuir model was more suitable to describe the Congo red adsorption than other models. Experimental data were analyzed using pseudo-first-order, pseudo-second-order, elovich and intra-particle kinetic models. It was found that kinetics followed a pseudo-second-order equation. Thermodynamic study showed that the adsorption was a exothermic process.

Keywords: Congo red; Carbon mesoporous; CMK-3; Adsorption; Equilibrium isotherm; Kinetic

1. Introduction

Among the different environmental pollutants, dyes are a large and important group of chemicals. They are widely used in different kinds of industries such as textile finishing, dyestuff manufacturing, carpet, plastics, paper and etc. These dyes are inevitably left in the industrial wastes and consequently discharged mostly in surface water resources. The discharge of colored wastewater into water resources even in a small amount can affect the aquatic life and food web. Since many organic dyes are harmful to human beings [1,2].

The methods for removal of color from industrial effluents include coagulation and flocculation [3], membrane separation [4], oxidation or ozonation [5], electro-coagulation [6], adsorption [7] and so on. Amongst the numerous techniques of dye removal, adsorption process is one of the effective techniques that have been successfully employed for color removal from wastewater.

A wide variety of materials, have been tested for the removal of dyes from aqueous solutions, including Activated carbon [8,9], zeolite [10], perlite [11], carbon

*Corresponding author.

nanotube [12], lemon peel [13] etc. However, most of these adsorbents either do not have considerable adsorption capacities or need relatively long adsorption contact times, for example, from several hours to a couple of days. Therefore, it is of interest to develop effective adsorbents with short contact times for the removal of toxic species from aqueous solutions.

There is an increasing demand for mesoporous materials as adsorbents [14–16], catalyst supports [17–19], gas separation [20,21], energy storage [22] and drug delivery [23]. Mesoporous carbon, CMK-3 is a fascinating material and exhibits a high surface area, a large pore volume, narrow pore size distribution, and well-ordered mesoporous structure [24,25]. These unique properties made CMK-3 as good candidate for adsorption of hazardous materials.

The main objective of the present work is to investigate the potential of CMK-3 as carbon mesoporous material for the removal of Congo red dye from aqueous solutions. Congo red (C.R.) with IUPAC name of sodium 3,3'-(1E,1'E)-biphenyl-4,4'-diylbis(diazene-2,1-diyl)bis(4-aminonaphthalene-1-sulfonate) (Fig. 1) is an important water-soluble anionic dye and its carcinogenic effects for human beings is known [26]. The affect of contact time, pH, initial concentration, and electrolyte on adsorption characteristics of CMK-3 was studied and the experimental data obtained from the equilibrium studies were fitted to Langmuir, Freundlich and temkin adsorption models. In addition, kinetic studies are also carried out to determine the the adsorption process.

2. Materials and methods

2.1. Materials

Triblock copolymer P123 ($EO_{20}PO_{70}EO_{20}$, EO = ethylene oxide, PO = propylene oxide, 5800) was supplied from Aldrich Co., and tetraethyl orthosilicate [TEOS, Si(OCH_2CH_4)4], sucrose, Congo red, NaCl, NaOH, HCl and ethanol were purchased from Merck (Germany).

2.2. Preparation of adsorbent

Mesoporous carbon material CMK-3 was prepared by using mesoporous silica material SBA-15 as hard template and sucrose as carbon source. SBA-15 was synthesized as reported by Zhao et al. [27]. In a typical synthesis, 2 g P123 was dissolved in 75 ml 2 mol l^{-1} HCl solution at 40°C and 4.16 g of tetraethyl orthosilicate was then added. After the solution was magnetically stirred at 40°C for 24 h, the mixture was transferred to an autoclave, which was kept at 100°C for 48 h under static condition. The resulting material was recovered by filtration and washing with distilled water. Subsequently, the sample was calcined at 550°C in air for 6 h to remove the organic template P123. Thus, SBA-15 was obtained.
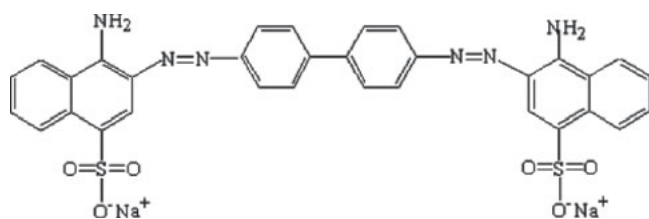
Mesoporous carbon, CMK-3, was prepared according to the process described by Jun et al. [28]. One gram of SBA-15 was added to 5 ml aqueous solution containing 1.25 g sucrose and 0.14 g H_2SO_4. The resulting sludge was heated in an oven at 100°C for 6 h and then 160°C for another 6 h. In order to obtain fully polymerized and carbonized sucrose inside the pores of the silica template, 5 ml aqueous solution containing 0.8 g sucrose and 0.09 g H_2SO_4 was added again and the mixture was subjected to the thermal treatment described above. Then, it was carbonized in an argon flow at 900°C for 6 h with a heating rate of 5°C min^{-1}. Finally, the mesoporous carbon (CMK-3) was obtained by removing the silica matrix using a 4 mol l^{-1} NaOH solution (50 vol% ethanol-50 vol% H_2O) at room temperature followed by filtration, washing, and drying at 120°C for 4 h.

2.3. Characterization of adsorbent

The textural properties of adsorbent were determined by using the nitrogen sorption technique. The nitrogen adsorption–desorption isotherms were measured at −196°C using a Micromeritics ASAP 2000 analyser. Prior to the measurement, sample degassed for 5 h at 70°C. The specific surface area was calculated according to the BET (Brunauer–Emmet and Teller) model [29], while the pore size and pore volume were calculated using the Barrett–Joyner–Halenda (BJH) formula [30] based on the desorption branch of the isotherm. The mesoporous structure of the sample was investigated using X-ray powder diffraction (XRD).The XRD patterns were obtained at room temperature on a Bruker D8 diffractometer with a CuKα (0.15406 nm) radiation source in the 2θ range from 0.5 to 5, with a step size of 0.02. Zeta potential of carbon sorbent (CMK-3) was measured at 25°C using a Zeta Meter (Lazer ZeeMeter Model 501, Pen Kem Inc.).

2.4. Adsorption studies

Batch experiments were carried out to evaluate the effect of contact time, initial dye concentration, solution pH, temperature and electrolyte for the removal of C.R. dye on CMK-3 adsorbent from aqueous solutions.

Fig. 1. Structure of Cango red (molecular formula: $C_{32}H_{22}N_6O_6S_2Na_2$).

In All experiments except for the initial concentration, 50 mg CMK-3 was added to 25 ml water solution of C.R. with a concentration of 1000 mg l^{-1}. After stirring on a shaker for predetermined time intervals, the solution was treated with centrifugation for solid–liquid separation. The residual concentration of dye solution was determined using a calibration curve prepared at the corresponding maximum wavelength (500 nm) using a UV–visible spectrometer (Unicol Instrument Co., Ltd.). The amount of adsorbed dye, Q (mg g^{-1}), was calculated by:

$$Q = \frac{(C_0 - C_e)V}{W} \tag{1}$$

where C_0 and C_e are the initial and equilibrium concentrations (mg l^{-1}), respectively, V is the volume of dye solution (l) and W is the weight (g) of CMK-3 adsorbent. The dye removal efficiencies under different conditions were calculated from the difference between the initial (without adsorbent) and equilibrium concentrations of the solution.

The effect of pH on dye removal was studied over a pH range of 3–9. The initial pH of the dye solution was adjusted by the addition of 1 mol l^{-1} solution of HCl or NaOH. The concentration of Congo red dye solution ranged from 50 to 1200 mg l^{-1} to investigate the adsorption isotherms. The sorption studies were also carried out at different temperatures (30°C, 40°C, 50°C and 60°C) to determine the effect of temperature on the adsorption process.

3. Result and discussion

3.1. Characterization of adsorbent

3.1.1. N_2 adsorption/desorption isotherm of carbon materials

As shown in Fig. 2, the N_2 adsorption/desorption isotherm of CMK-3 is a type IV curve of mesoporous materials with a steep hysteresis loop. The sharp rise at relative pressure (P/P_0) of about 0.4 indicates the existence of mesopores with narrow pore size distribution [25]. According to BET method, the specific surface area (S_{BET}) and pore volume are estimated to be 918 m^2 g^{-1} and 0.7557 m^3 g^{-1}, respectively. The CMK-3 obtained from SBA-15 possesses pores with average diameter of 3.64 nm.

3.1.2. Powder X-ray diffractometry

The low angle XRD patterns of the SBA-15 and CMK-3 are shown in Fig. 3. For SBA-15, three well-resolved peaks with 2θ at 0.82, 1.46, and 1.7, indexed as (100), (110), and (200) reflections associated with
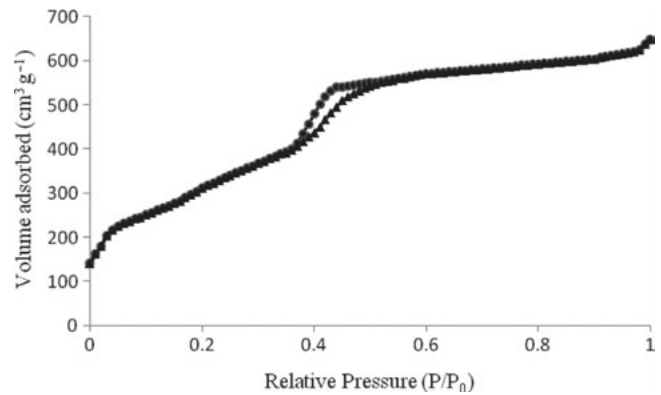
Fig. 2. Nitrogen adsorption–desorption isotherm of CMK-3.
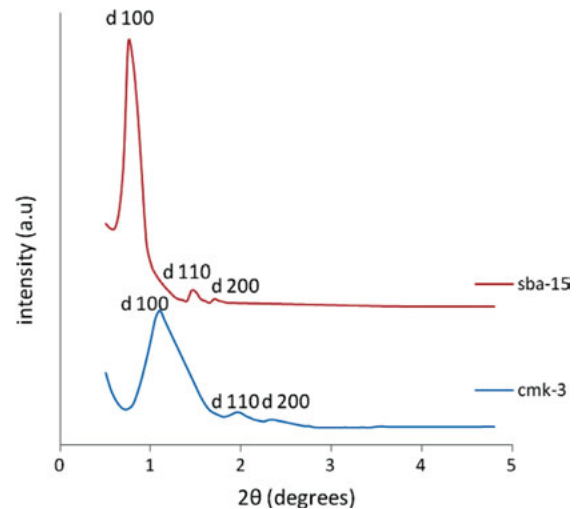
Fig. 3. Low-angle X-ray diffraction patterns of SAB-15 and CMK-3.

$p6mm$ hexagonal symmetry, were observed, indicative of the well-ordered mesoporous structure of SBA-15. The XRD patterns of CMK-3 also gave a strong (100) peak and weak (110) and (200) reflection peaks similar to the $p6mm$ hexagonal symmetry of the SBA-15 template. This indicates that CMK-3 is a perfect replica of SBA-15 [24,28].

3.1.3. pH at the point of zero charge

For any particular adsorbent, the pH at the zero point charge is a characteristic that determines the pH at which the surface has net electrical neutrality. In this work, Zeta potential of the CMK-3 sample was measured in a wide range of pH. As shown in Fig. 4, measurements indicate that this material has a zero charge at
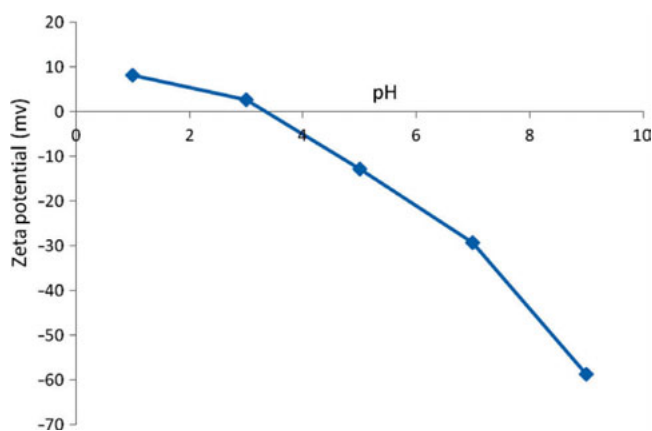
Fig. 4. Zeta potential-pH profile of CMK-3.

pH 3.3 and positive surface of adsorbent, at pH values below the zero point.

3.2. Study of important parameters on the adsorption of Cango red dye by CMK-3 adsorbent

3.2.1. Effect of contact time

The effect of contact time for the adsorption of Congo red dye on CMK-3 was investigated for a period of 2 h for initial dye concentration of 1000 mg l^{-1}. As seen in Fig. 5, it is evident that time has significant influence on the adsorption of dye. It can be seen that the adsorption of Congo red dye was quite rapid in the first 30 min, then gradually increased with the prolongation of contact time. After 60 min of contact, no obvious variation in dye adsorbed was examined. Based on these results, 60 min was taken as the equilibrium time in batch adsorption experiments.
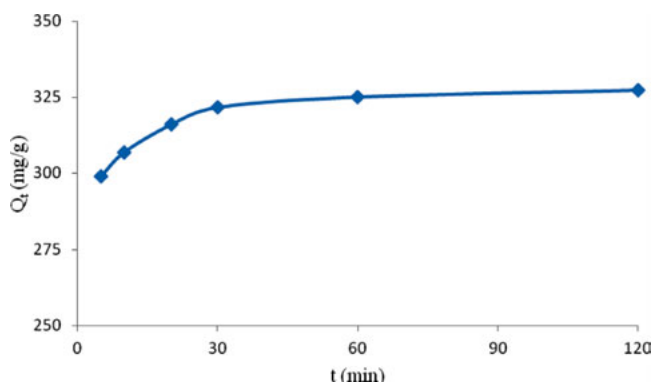
Fig. 5. Effect of contact time on removal of C.R. dye by CMK-3 (initial dye concentration: 1000 mg l^{-1}, cmk-3 dosage: 50 mg [25 ml]$^{-1}$).

3.2.2. Effect of pH

To study the influence of solution pH on the adsorption capacities of CMK-3 for Congo red dye at equilibrium conditions, experiments were carried out using various initial pHs varying from 3 to 9. As shown in Fig. 6, the amount of adsorption of solute increases as the pH is decreasing. When the pH is changed from 3 to 9, the adsorption will decrease from 361 to 317 mg g^{-1}. Higher adsorptions at lower pH values could be well explained by protonation properties of the adsorbent. At pHs below the zero point charge (pHs < 3.3), that is, higher hydrogen ion concentration, the negative charges at the surface of internal pores are neutralized and some more new adsorption sites were developed because the surface provided a positive charge for anionic Cango red dye to get adsorbed. A similar type of behavior is also reported for the adsorption of the dye at different adsorbents [31].

3.2.3. Effect of initial dye concentration

The adsorption experiments were carried out in initial dye concentration range of 50–1200 mg l^{-1}. Fig. 7
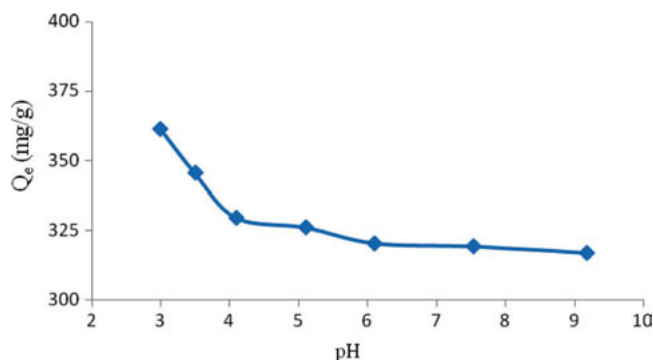
Fig. 6. Effect of pH on removal of C.R dye by cmk-3 (initial dye concentration: 1000 mg l^{-1}, CMK-3 dosage: 50 mg [25 ml]$^{-1}$).
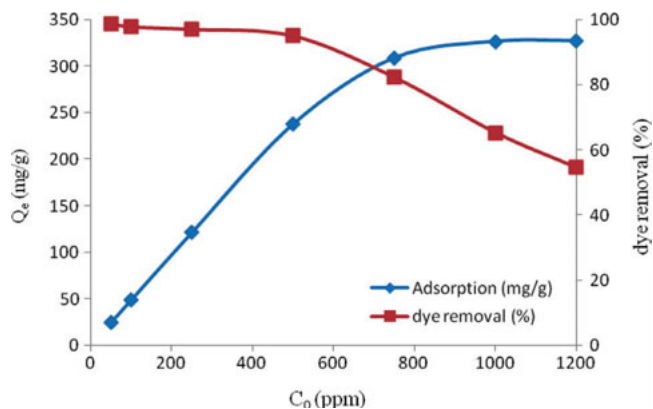
Fig. 7. Effect of initial dye concentration on removal of C.R. dye by CMK-3.

shows the effect of the initial concentration on the amount of adsorption and dye removal efficiency. It was observed that dye removal efficiency reached up to 99% at lower concentration (50 mg l^{-1}), then decreased to 54% at higher concentration (1200 mg l^{-1}). Dye removal efficiency was higher for low initial concentration because of availability of unoccupied binding sites on the adsorbents. Percent color removal decreased with increasing dye concentration because of nearly complete coverage of the binding sites at high dye concentration. In contrast, the amount of dye adsorbed was found to increase with increasing initial concentration of dyes. When the dye concentration was increased, the sorption capacity at equilibrium increased from 24.66 to 326.5 mg g^{-1} with an increase in the initial concentration from 50 to 1200 mg l^{-1}. This is attributable to the increase in the driving force of the concentration gradient with the higher initial dye concentration.

3.2.4. Effect of electrolyte (sodium chloride) concentration

Wastewaters that contain dyes commonly include significant quantities of salts, thus the effect of electrolyte on C.R. removal needs to be investigated. Fig. 8 illustrates the effect of NaCl on the amount of C.R. at an initial CR concentration of 1000 mg l^{-1} at 30°C and solution pH. It can be seen that adsorption of C.R. increased with increasing NaCl concentration. The presence of electrolyte may have two opposite effects. First, they may cause the neutralization of surface charge of adsorbent while competing with dye for surface adsorption. With the increasing ionic strength, the adsorption capacity decreases due to screening of the surface charges. Secondly, adding salt to the solution decreases the dissociation of dye molecules to their ionic forms and hence dye molecules as dominant species in the solution extract to carbon phase so rapidly because the extraction of a nonionic compound to an organic phase is much easier than its ionic form.

The second effect seems to be dominant in this case and causes higher degree of dye adsorption on mesoporous adsorbent [32].

3.2.5. Effect of temperature on the adsorption

Fig. 9 shows the maximum adsorption capacity of C.R. on the prepared material versus the temperature. It was found that the adsorption capacity decreased from 326 to 314 mg g^{-1} with increase in temperature from 30°C to 60°C, indicating the exothermic nature of the adsorption reaction. It can be explained that as temperature increased, the physical bonding between the dye molecules and the active sites of the adsorbent weakened. In addition, the solubility and dissociation of C.R. dye also increased and adsorbate–adsorbent interactions decreased. Therefore the solute was more difficult to adsorb at higher temperature. A similar bevaviour also showed by Tahir and Rauf [33].

3.3. Adsorption isotherms

For solid–liquid system, the equilibrium of sorption is one of important physico-chemical aspects in description of adsorption behavior. In this work, three well-known models of Langmuir, Freundlich and Temkin isotherms are evaluated.

The Langmuir isotherm assumes monolayer adsorption onto a surface containing a finite number of adsorption sites with no transmigration of the adsorbate in the plane of the surface [34]. This model is the most widely used two-parameter equation, generally expressed in the form by the following equation:

$$\frac{C_e}{Q_e} = \frac{1}{Q_m K_L} + \frac{1}{Q_m} C_e \tag{2}$$

Fig. 8. Effect of electrolyte on removal of C.R. dye by CMK-3 (initial dye concentration: 1000 mg l^{-1}, cmk-3: dosage 50 mg [25 ml]$^{-1}$).
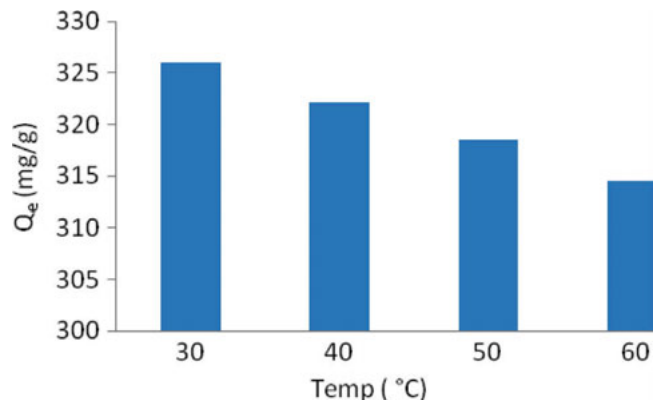
Fig. 9. Maximum adsorption capacity of C.R. dye on the CMK-3 versus temperature.

where C_e is the equilibrium concentration of the adsorbate (mg l^{-1}), Q_e is the amount of adsorbate adsorbed per unit mass of adsorbent (mg g^{-1}), K_L the Langmuir adsorption constant (l mg^{-1}), and Q_m is the theoretical maximum adsorption capacity (mg g^{-1}).

The essential characteristic of Langmuir equation can be expressed in terms of a dimensionless separation factor R_L, which is defined as:

$$R_L = \frac{1}{1 + K_L C_0} \tag{3}$$

where k_l is the Langmuir isotherm constant (l mg^{-1}) and C_0 is the initial dye concentration (mg l^{-1}). The R_L value indicates the type of the isotherm to be either favorable ($0 < R_L < 1$), unfavorable ($R_L > 1$), linear ($R_L = 1$) or irreversible ($R_L = 0$).

The Freundlich isotherm in the other hand takes heterogeneous systems into account and is not restricted to the formation of the monolayer [35]. The well-known logarithmic form of the Freundlich isotherm is given by the following equation:

$$\ln Q_e = \ln k_F + \left(\frac{1}{n}\right) \ln C_e \tag{4}$$

where K_f (l mg^{-1}) and n are Freundlich constants. K_F can be defined as an adsorption or distribution coefficient and represents the amount of adsorbate adsorbed on an adsorbent for a unit equilibrium concentration while n giving an indication of how favorable the adsorption process. The slope of $1/n$ ranging between 0 and 1 is a measure of adsorption intensity or surface heterogeneity, becoming more heterogeneous as its value gets closer to zero. A value for $1/n$ below one indicates a normal Langmuir isotherm while $1/n$ above one is indicative of cooperative adsorption [36].

The Temkin isotherm model [37] contains a factor that explicitly takes into account adsorbing species-adsorbate interactions. This model assumes the following: (i) the heat of adsorption of all the molecules in the layer decreases linearly with coverage due to adsorbent–adsorbate interactions, and that (ii) the adsorption is characterized by a uniform distribution of binding energies, up to some maximum binding energy. The derivation of

the Temkin isotherm assumes that the fall in the heat of sorption is linear rather than logarithmic, as implied in the Freundlich equation. The Temkin isotherm has commonly been applied in the following form:

$$Q_e = B_T \ln K_T + B_T \ln C_e \tag{5}$$
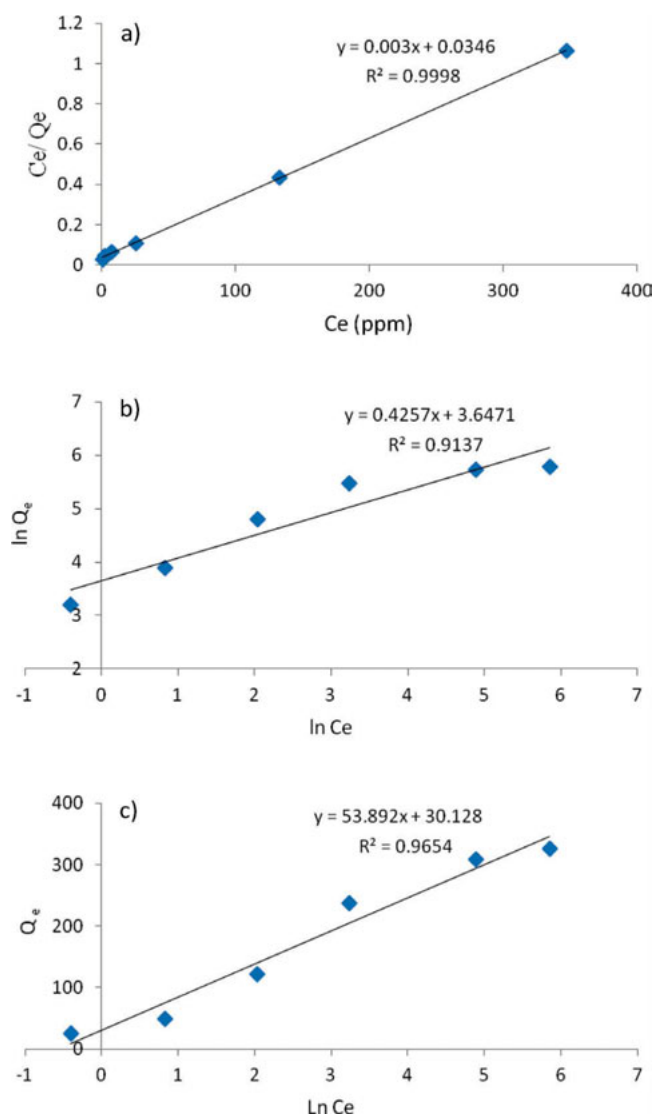
Fig. 10. Experimental, (a) Langmuir, (b) Freundlich and (c) Temkin isotherms for adsorption of of C.R. on CMK-3.

Table 1
Langmuir, Freundlich and Temkin constants for the adsorption of C.R. on CMK-3

Langmuir				Freundlich			Temkin		
Q_m	K_L	R_L	R^2	K_F	$1/n$	R^2	K_T	B	R^2
333.3	0.087	0.011–0.187	0.9998	38.35	0.4257	0.9137	1.75	53.89	0.9654

where, K_T and B_T are the Temkin isotherm constants. The isotherm constant K_T is the equilibrium binding constant (l mg^{-1}) corresponding to the maximum binding energy and constant B_T is related to the heat of adsorption.

Langmuir, Freundlich and Temkin isotherms for the Congo red CMK-3 system are shown in the Fig. 10. Isotherm parameters and the Correlation coefficients, R^2, were calculated and summarized in Table 1. As shown in the table, the Langmuir isotherm with correlation coefficient of 0.9998 represents a better fit of experimental data than Freundlich and Temkin models with correlation coefficient of 0.913. It indicates that monolayer adsorption of C.R. dye takes place on the homogeneous surface of mesoporous carbon adsorbent. The amount of computed maximum monolayer capacity for removal of C.R. from aqueous media by Langmuir model found to be 326 mg g^{-1}. Moreover, the values of the dimensionless constant R$_L$ (0.011–0.187) indicate that the adsorption is favorable and rather irreversible. As seen from Table 1, the value of 1/n was also found to be between 0 and 1, indicating the high adsorption intensity.

3.4. Adsorption kinetics

It is important to be able to predict the rate at which a solute is removed from aqueous solutions in order to design an adsorption treatment plant. Adsorption rate constant for the C.R. dye was determined by using pseudo-first-order, pseudo-second-order, elovich and intr-aparticle diffusion models. The conformity between the experimental data and the model-predicted values was expressed by the correlation coefficients (r^2). A relatively high correlation coefficients value indicates that the model successfully describes the kinetics of the dye adsorption.

A pseudo-first-order equation can be expressed in a linear form as [38]:

$$In(Q_e - Q_t) = In\ Q_e - k_1\ t \tag{6}$$

where q_e and q_t are the amount of dye adsorbed (mg g^{-1}) on the adsorbents at the equilibrium and at time t, respectively, and k_1 is the rate constant of adsorption (min^{-1}). Values of k_1 were calculated from the plots of log(q_e-q_t) versus t for different concentrations of the dye.

The pseudo-second-order kinetic model is expressed by the following equation [39]:

$$\frac{t}{Q_t} = \frac{1}{k_2 Q_e^2} + \frac{1}{Q_e}\ t \tag{7}$$

where k_2 (g.mg^{-1}.min^{-1}) is the rate constant of the pseudo-second-order model. This model is based on the

assumption that the rate-limiting step involves chemisorption of adsorbate on the adsorbent.

In reactions involving chemisorption of adsorbates on a solid surface without desorption of the products, the rate decreases with time due to an increased surface coverage. One of the most useful models for describing such adsorption is the Elovich equation [40]:

$$Q_t = A + B\ ln\ t \tag{8}$$

where q_t (mg.g^{-1}) is the amount of adsorption at equilibrium and at time t.

The intra-particle diffusion model [41] has been applied to gain a deeper knowledge about the mechanism of dye adsorption onto mesoporous carbon. In this model, described by Eq. (9), the intra-particle diffusion is considered as a rate-limiting step:

$$Qt = k_i\ t^{1/2} \tag{9}$$

where q_t and k_i are the amount adsorbed at time t (mg g^{-1}) and intra-particle rate constant (mg g^{-1} min$^{1/2}$), respectively. Such a plot may present multi-linearity, indicating that a few steps take place. The first, sharper portion is attributed to the diffusion of adsorbate through the solution to the external surface of adsorbent or the boundary layer diffusion of solute molecules. The second portion describes the gradual adsorption stage, where intra-particle diffusion rate is rate-limiting. The third portion is the final equilibrium stage, where the intra-particle diffusion starts to slow down due to the extremely low solute concentration in solution [42].

The applicability of the kinetic models is checked by constructing linear plots of selected models (Fig. 11). The results from fitting experimental data with selected kinetic models are presented in Table 2. The correlation coefficient for the pseudo-first-order kinetic model was low. Moreover, a large difference of equilibrium adsorption capacity (q_e) between the experiment and calculation was observed, indicating a poor pseudo-first-order fit to the experimental data. Therefore, the kinetic data was also fitted with pseudo-second-order and elovich models. As the Figs. 11(b and c) and Table 2 clearly show, the pseudo-second order and elovich models, respectively, with correlation coefficients of 0.9996 and 0.9886 better than the pseudo first-order model explain the absorption process; therefore the sorption of C.R dye on carbonaceous material can be described by chemisorption. Compared with elovich model, the pseudo second order model has a larger correlation coefficient and the calculated adsorption capacity agrees reasonably well with the experimental data. This suggests that the adsorption system studied belongs to the second-order kinetic model, based on the assumption that
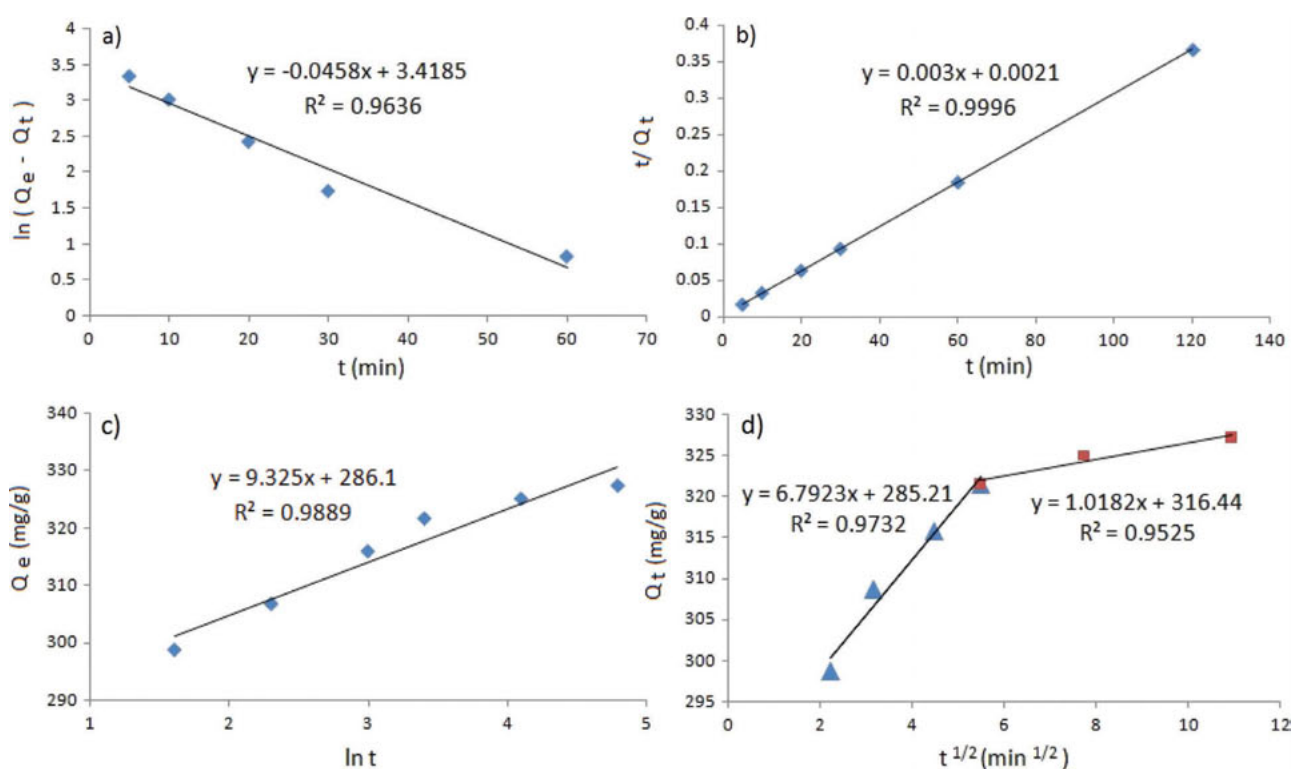
Fig. 11. (a) Pseudo-first order, (b) pseudo-second order, (c) elovich, (d) intraparticle diffusion kinetic models for adsorption of C.R. on CMK-3.

Table 2
Pseudo-first-order, pseudo-second-order, elovich and intraparticle diffusion kinetic models constants for the adsorption of C.R. on CMK-3

Pseudo-first-order			Pseudo-second-order			Elovich			Intra-particle diffusion			
k_1 (min^{-1})	R^2	Q_e	k_2 (g mg^{-1} min^{-1})	R^2	Q_e	A	B	R^2	k_i1 (mg g^{-1} min$^{-1/2}$)	$R_1{}^2$	k_i2 (mg g^{-1} min$^{-1/2}$)	$R_2{}^2$
0.0458	0.9636	30.53	0.0043	0.9996	333.3	9.32	286.1	0.9889	6.79	0.9732	1.02	0.9525

the rate-limiting step may be chemical adsorption or chemisorption.

Fig. 11d. shows the plot of fractional uptake for C.R. versus square root of time. It can be observed that the plot is not linear over the whole time range and has two linear portions. The two phases in the intra-particle diffusion plot suggests that the sorption process proceeds by firstly surface sorption and then the intra-particle diffusion. The initial linear portion is attributed to bulk diffusion while the second linear portion is due to intra-particle or pore diffusion. At the beginning of adsorption process, the dye was adsorbed by the exterior surface of CMK-3 particles, so the adsorption rate was very fast. When the adsorption of the exterior surface reached saturation, the dye molecules entered into the pores of CMK-3 and were adsorbed by the interior surface of the adsorbent. With decrease of the dye concentration in the solution, the diffusion rate became lower and lower, the diffusion processes reached the final equilibrium stage. Therefore, the changes of $k_{i,1}$ and $k_{i,2}$ could be attributed to the adsorption stages of the exterior surface and interior surface, respectively. Since $k_{i,1}$ values for first part of plot is high, this step is not rate limiting step, therefore, the rate limiting step in adsorption process is intra-particle diffusion due to low $k_{i,2}$ value.

4. Conclusions

Ordered mesoporous carbon (CMK-3) was successfully prepared using silica SBA-15 as hard template.

N_2 adsorption and XRD results demonstrate that the synthesized material is a good replica of SBA-15 and its specific surface area and average pore diameter found to be 918 m^2 g^{-1} and 3.64 nm respectively. Batch adsorption of Congo red dye on the mesoporous carbon indicated that the adsorption process is fast enough, as maximum removal took place within 60 min of contact time and removal efficiency of dye was improved in acidic solutions. The adsorption of dye increased with increasing initial dye concentration and salt concentration. Fitting equilibrium data to Langmuir, Freundlich and Temkin isotherms showed that Langmuir model was more suitable to describe the Congo red adsorption with maximum monolayer adsorption capacity of 333.3 mg g^{-1}. The adsorption kinetics was found to follow closely the pseudo-second-order kinetic model. The maximum adsorption capacity decreased with increasing temperature.

Acknowledgements

References

[1] J. Karthikeyan, Pollution management in industries, Environmental Publication-Karda, India, 1988.
[2] T. Robinson, B. Chandran and P. Nigam, Removal of dyes from a synthetic textile dye effluent by biosorption on apple pomace and wheat straw, Water Res., 36 (2002) 2824–2830.
[3] J. Panswed and S. Wongchaisuwan, Mechanism of dye wastewater color removal by magnesium carbonate-hydrated basic, Water Sci. Technol., 18 (1986) 139–144.
[4] H. Jirankova, J. Mrazek, P. Dolecek and J. Cakl, Organic dye removal by combined adsorption–membrane separation process, Desalin. Water Treat., 20 (2010) 96–101.
[5] P.K. Malik and S.K. Saha, Oxidation of direct dyes with hydrogen peroxide using ferrous ion as catalyst, Sep. Purif. Technol., 31 (2003) 241–250.
[6] A. Alinsafi, M. Khemis, M.N. Pons, J.P. Leclerc, A. Yaacoubi and A. Benhammou, Electro-coagulation of reactive textile dyes and textile wastewater, Chem. Eng. Process., 44 (2005) 461–470.
[7] D. Sun, X. Zhang, Y. Wu and X. Liu, Adsorption of anionic dyes from aqueous solution on fly ash, J. Hazard. Mater., 181 (2010) 335–342.
[8] S.J. Allen, Use of adsorbents for the removal of pollutants from wastewaters: Types of adsorbent materials, CRC, Boca Raton, FL, 1996.
[9] K.Y. Foo and B.H. Hameed, An overview of dye removal via activated carbon adsorption process, Desalin. Water Treat., 19 (2010) 255–274.
[10] V. Meshko, L. Markovska, M. Mincheva and A.E. Rodrigues, Adsorption of basic dyes on granular activated carbon and natural zeolite, Water Res., 35 (2001) 3357–3366.
[11] M. Dogan and M. Alkan, Adsorption kinetics of methyl violet onto perlite, Chemosphere, 50 (2003) 517–528.
[12] K. Nadafi, A. Mesdaghinia, R. Nabizadeh, M. Younesian and M. Jahangiri Rad, The combination and optimization study on RB29 dye removal from water by peroxy acid and single-wall carbon nanotubes, Desalin. Water Treat., 27 (2011) 237–242.
[13] K.V. Kumar, Optimum sorption isotherm by linear and non-linear methods for malachite green onto lemon peel, Dyes Pigm., 74 (2007) 595–597.
[14] M. Anbia and S. Ershad Moradi, CTAB modified nanoporous carbon for the adsorption of chromate ions from industrial wastewater, Desalin. Water Treat., 21 (2010) 44–52.
[15] X. Sun, C. Hu and J. Qu, Adsorption and removal of arsenite on ordered mesoporous Fe-modified ZrO2, Desalin. Water Treat., 8 (2009) 139–145.
[16] M. Anbia, N. Mohammadi and K. Mohammadi, Fast and efficient mesoporous adsorbents for the separation of toxic compounds from aqueous media, J. Hazard. Mater., 176 (2010) 965–972.
[17] G. Wang, G. Liu, M. Xu, Z. Yang, Z. Liu, Y. Liu, S. Chen and L. Wang, Ti-MCM-41 supported phosphotungstic acid: An effective and environmentally benign catalyst for epoxidation of styrene, Appl. Surf. Sci., 255 (2008) 2632–2640.
[18] A. Taguchi and F. Schüth, Ordered mesoporous materials in catalysis, Microporous. Mesoporous. Mater., 77 (2005) 1–45.
[19] K. Iwanami, T. Sakakura, H, Yasuda and H. Yasuda, Efficient catalysis of mesoporous Al-MCM-41 for Mukaiyama aldol reactions, Catal. Commun., 10 (2009) 1990–1994.
[20] K.N.M. Miyamoto, Y. Fujioka and K. Yogo, Hydrogen separation membrane encapsulating Pd nanoparticles in a silica layer, Desalin. Water Treat., 17 (2010) 233–241.
[21] B. Zornoza, P. Gorgojo, C. Casado, C. Tellez and J. Coronas, Mixed matrix membranes for gas separation with special nanoporous fillers, Desalin. Water Treat., 27 (2011) 42–47.
[22] M.S. Park, G.X. Wang, Y.M. Kang, S.Y. Kim, H.K. Liu and S.X. Dou, Mesoporous organo-silica nanoarray for energy storage media, Electrochem. Commun., 9 (2007) 71–75.
[23] I.I. Slowing, J.L. Vivero-Escoto, C.W. Wu and V.S.Y. Lin, Adv. Mesoporous silica nanoparticles as controlled release drug delivery and gene transfection carriers, Drug Delivery Rev., 60 (2008) 1278–1288.
[24] J. He, K. Ma, J. Jin, Z. Dong, J. Wang and R. Li, Preparation and characterization of octyl-modified ordered mesoporous carbon CMK-3 for phenol adsorption, Microporous. Mesoporous. Mater., 121 (2009) 173–177.
[25] J. Yu, W. Du, F. Zhao and B. Zeng, High sensitive simultaneous determination of catechol and hydroquinone at mesoporous carbon CMK-3 electrode in comparison with multi-walled carbon nanotubes and Vulcan XC-72 carbon electrodes, Electrochim. Acta., 54 (2009) 984–988.
[26] E. Lorenc-Grabowska and G. Gryglewicz, Adsorption characteristics of Congo red on coal-based mesoporous activated carbon, Dyes Pigm., 74 (2007) 34–40.
[27] D. Zhao, J. Feng, Q. Huo, N. Melosh, G.H. Fredrickson and B.F. Chmelka, Triblock copolymer syntheses of mesoporous silica with periodic 50 to 300 angstrom pores, Science, 279 (1998) 548–552.
[28] S. Jun, S.H. Joo, R. Ryoo, M. Kruk, M. Jaronice and Z. Liu, Synthesis of new, nanoporous carbon with hexagonally ordered mesostructure, J. Am. Chem. Soc., 122 (2000) 10712–10713.
[29] S. Brauner, P.H. Emmet and E. Teller, Adsorption of gases in multimolecular layers, J. Am. Chem. Soc., 60 (1938) 309–319.
[30] E.P. Barrett, L.G. Joyner and P.P. Halenda, The determination of pore volume and area distribution in porous substances. I. Computations from nitrogen isotherms, J. Am. Soc., 73 (1951) 373–380.
[31] G. Vijayakumar, M. Dharmendirakumar, S. Renganathan, S. Sivanesan and G. Baskar, Removal of Congo red from aqueous solutions by Perlite, Clean, 37 (2009) 355–364.
[32] A. Riga, K. Soutsas, K. Ntampegliotis, V. Karayannis and G. Papapolymerou, Effect of system parameters and of inorganic salts on the decolorization and degradation of Procion Hexl dyes, Desalination, 211 (2007) 72–86.
[33] S.S. Tahir and N. Rauf, Removal of cationic dye from aqueous solutions by adsorption onto bentonite clay, Chemosphere, 63 (2006) 1842–1848.
[34] I. Langmuir, The constitution and fundamental properties of solids and liquids, J. Am. Chem. Soc., 38 (1916) 2221–2295.
[35] T.W. Weber and R.K. Chakkravorti, Pore and solid diffusion models for fixedbed adsorbers, AIChE J., 20 (1974) 228–234.

[36] K. Fytianos, E. Voudrias and E. Kokkalis, Sorption–desorption behavior of 2,4-dichloriphenol by marine sediments, Chemosphere, 40 (2000) 3–6.

[37] M.J. Temkin and V. Pyzhev, Recent modifications to Langmuir isotherms, Acta Physicochim. URSS, 12 (1940) 217–22.

[38] S. Lagergren and K. Svenska, About the theory of so called adsorption of soluble substances, Veternskapsakad Handl., 24 (1898) 1–6.

[39] Y.S. Ho and G. McKay, Sorption of dye from aqueous solution by peat, Chem. Eng. J., 70 (1998) 115–124.

[40] S.H. Chien and W.R. Clayton, Application of Elovich equation to the kinetics of phosphate release and sorption on soils, Soil Sci. Soc. Am. J., 44 (1980) 265–268.

[41] W.J. Weber and J.C. Morris, Kinetics of adsorption of carbon from solutions, J. Sanit. Eng. Div. Am. Soc. Civ. Eng., 89 (1963) 31–63.

[42] M.S. Chiou and G.S. Chuang, Competitive adsorption of dyemetanil yellowandRB15 in acid solutions on chemically cross-linked chitosan beads, Chemosphere, 62 (2006) 731–740.